Coastal Engineering Journal

ISSN: 2166-4250 (Print) 1793-6292 (Online) Journal homepage: http://www.tandfonline.com/loi/tcej20

Improved Boussinesq-type equations for spatially and temporally varying bottom

S. Beji

To cite this article: S. Beji (2018) Improved Boussinesq-type equations for spatially and temporally varying bottom, Coastal Engineering Journal, 60:3, 318-326, DOI: 10.1080/21664250.2018.1520796

To link to this article: https://doi.org/10.1080/21664250.2018.1520796

Published online: 20 Sep 2018.

COASTAL ENGINEERING JOURNAL
2018, VOL. 60, NO. 3, 318–326
https://doi.org/10.1080/21664250.2018.1520796

ORIGINAL RESEARCH PAPER

Improved Boussinesq-type equations for spatially and temporally varying bottom

S. Beji

Faculty of Naval Architecture and Ocean Engineering, Istanbul Technical University, Istanbul, Turkey

ABSTRACT
Boussinesq-type equations with improved linear dispersion characteristics are derived for spatially and temporally varying bottom. Starting from the first principles, spatial variations and temporal movements of seabed due to underwater earthquakes, landslides and alike are incorporated into the Boussinesq-type equations. The momentum equation is then manipulated by the partial replacement technique so that a generalized Boussinesq set of equations with improved dispersion characteristics is obtained. For an impulsive bed motion-simulated wave profiles are compared with experimental measurements. Waves generated by an ellipsoidal slump moving down on an inclined plane are also numerically simulated to disclose the effect of a newly derived term. Overall, the new set of equations is expected to provide more accurate representation of wave motions due to bottom movements by correctly modeling accelerative bed effects and propagation of relatively shorter waves.

ARTICLE HISTORY
Received 25 January 2018
Accepted 20 August 2018
Published online 20 September 2018

KEYWORDS
Boussinesq equations; spatially and temporally varying bottom; improved dispersion characteristics; landslides and tsunamis

1. Introduction

Mei and Le Méhauté (1966) and shortly afterwards Peregrine (1967) derived Boussinesq-like equations (Boussinesq, 1872) for water of spatially varying depth. Peregrine's model, being formulated in terms of vertically averaged or mean velocity, has since then become virtually standard Boussinesq model of the coastal engineering community. Witting (1984) gave a highly nonlinear set of Boussinesq-like equations based on a new velocity concept that also extended the applicable range of equations to greater relative water depths. Following a different approach, Madsen, Murray, and Sørensen (1991) derived new Boussinesq-type equations with better dispersion characteristics. Madsen and Sørensen (1992) carried the derivation a step further to varying bathymetry. Nwogu (1993) used the velocity at an arbitrary depth for deriving alternative Boussinesq-type equations. This concept was indeed quite in line with that of Witting (1984) but physically more meaningful. Beji and Nadaoka (1996) followed an approach similar to Madsen and Sørensen (1992) to produce a Boussinesq-type wave model with consistent shoaling properties for spatially varying depth. Much more elaborated works have followed to further improve dispersion and nonlinear characteristics of Boussinesq-type equations; Madsen and Schäffer (1998) gave a very detailed account with their own contributions.

Recent decades have seen considerable increase in capabilities of computational facilities, which in turn provided augmented capacities for numerical simulation of global scale wave events such as tsunamis and underwater landslides. Among relatively earlier works Shuto (1991) presented a comprehensive review with emphasis on numerical aspects of modeling while Nagano, Imamura, and Shuto (1991) gave an oceanic propagation model and its application for a particular case. Quite detailed programming aspects of a numerical tsunami model can be found in Goto, Ogawa, and Imamura (1997). Watts (2000) studied the tsunami generation aspects of a sliding solid block. In the same vein, impulsive waves generated by landslides were experimentally investigated by Fritz, Hager, and Minor (2004). A global scale numerical modeling of the catastrophic Indonesian tsunami of 2004 was reported in Kowalik and Logan (2005). Dispersive aspects of waves for the Indonesian tsunami was considered by Horrillo, Kowalik, and Shigihara (2006). Yamazaki, Cheung, and Kowalik (2010) developed a non-hydrostatic global tsunami model and gave its numerical treatment with applications. A work on accurate specification of tsunami source characteristics was reported by An, Sepúlveda, and Liu (2014). Literature concerning the simulation of surface waves generated by underwater earthquakes or landslides is extensive; the reader is directed to Titov, Kanoglu, and Synolakis (2016), where a very recent state-of-the-art review with an extensive list of references can be found.

In this work a Boussinesq-type wave model for a bathymetry comprising not only spatial but also temporal variations is developed based on the first

CONTACT S. Beji sbeji@itu.edu.tr

principles. The resulting equations, which may be viewed as generalized forms of Peregrine's equations for time-dependent depths, as given in Wu (1979) and Wu (1981), are further manipulated by the partial replacement technique of Beji and Nadaoka (1996) to obtain another set of equations with improved dispersion characteristics as well as time-dependent bathymetry. The model equations are capable of simulating relatively short dispersive waves generated by temporal bottom movements due to underwater earthquakes or landslides. The performance of equations is tested against time history records of Hammack (1973) for an impulsive bed movement. A hypothetical 2D (physically 3D) simulation of waves generated by an elliptic slump is considered to reveal the effect of a newly derived term comprising bottom acceleration in the momentum equation.

2. Mathematical derivation

The derivation is carried out by integrating the continuity and momentum equations vertically from the seabed to the free surface. The final equations are expressed in terms of vertically averaged or mean horizontal velocity vector as this choice, besides being rather conventional, renders the continuity equation exact. Use of an exact mass conservation equation is quite advantageous for obtaining accurate numerical solutions.

2.1. Continuity equation

The conservation of mass or the continuity equation for an incompressible homogeneous fluid can be written as

$$\nabla \cdot \mathbf{u} + \frac{\partial w}{\partial z} = 0 \tag{1}$$

where $\mathbf{u}$, w are respectively the horizontal velocity vector and vertical velocity component. A bold face symbol indicates a vector with $x-$ and $y-$ components only, that is, $\mathbf{u} = (u, v)$; the two-dimensional gradient operator, $(\partial/\partial x, \partial/\partial y)$, is denoted by ∇.

Before carrying out the vertical integration in the $z-$direction, it is recalled that if a surface deforming in time, $S(x, y, z, t)$, is a material surface it satisfies $DS/Dt = 0$ where $D/Dt = \partial/\partial t + u\partial/\partial x + v\partial/\partial y + w\partial/\partial z$ is the material derivative operator. Then, for a domain bounded above by the free surface $S_f(x, y, z, t) = z - \zeta(x, y, t)$ and bounded below by a bed $S_b(x, y, z, t) = z + h(x, y, t)$, the kinematic surface conditions are respectively expressed as

$$\frac{DS_f}{Dt} = \frac{D}{Dt}[z - \zeta(x, y, t)] = w - \zeta_t - \mathbf{u} \cdot \nabla\zeta = 0 \quad \text{on} \quad z = \zeta(x, y, t) \tag{2}$$

$$\frac{DS_b}{Dt} = \frac{D}{Dt}[z + h(x, y, t)] = w + h_t + \mathbf{u} \cdot \nabla h = 0 \quad \text{on} \quad z = -h(x, y, t) \tag{3}$$

From the above formulations it is understood that the origin of the $z-$axis is taken at the still water level $z = 0$ and the seabed lies below it while $h(x, y, t)$ is always a positive quantity denoting the local water depth at any given horizontal location and instant.

Integrating now Equation (1) from the seabed $z = -h(x, y, t)$ to the free surface $z = \zeta(x, y, t)$ results in

$$\int_{-h}^{\zeta} (\nabla \cdot \mathbf{u}) dz + \int_{-h}^{\zeta} \frac{\partial w}{\partial z} dz = 0 \tag{4}$$

Recalling Leibnitz's rule for differentiation of integrals in connection with the first term in Equation (4) gives

$$\nabla \cdot \left(\int_{-h}^{\zeta} \mathbf{u}\, dz \right) = \int_{-h}^{\zeta} (\nabla \cdot \mathbf{u}) dz + \mathbf{u}_\zeta \cdot \nabla\zeta + \mathbf{u}_{-h} \cdot \nabla h \tag{5}$$

where a subscript denotes the variable at which u is evaluated for z. The integration of the second term in Equation (4) gives $w_\zeta - w_{-h}$, then with the use of Equation (5), Equation (4) becomes

$$\nabla \cdot \left(\int_{-h}^{\zeta} \mathbf{u}\, dz \right) + w_\zeta - \mathbf{u}_\zeta \cdot \nabla\zeta - w_{-h} - \mathbf{u}_{-h} \cdot \nabla h = 0 \tag{6}$$

Using $w_\zeta = \zeta_t + \mathbf{u}_\zeta \cdot \nabla\zeta$ from Equation (2) and $w_{-h} = -h_t - \mathbf{u}_{-h} \cdot \nabla h$ from Equation (3) results in

$$\zeta_t + h_t + \nabla \cdot \left(\int_{-h}^{\zeta} \mathbf{u}\, dz \right) = 0 \tag{7}$$

The mean or the vertically averaged horizontal velocity vector is defined as

$$\bar{\mathbf{u}} = \frac{1}{(h + \zeta)} \int_{-h}^{\zeta} \mathbf{u}\, dz \tag{8}$$

In terms of the mean velocity vector the vertically integrated continuity equation for spatially and temporally varying depth becomes

$$\zeta_t + h_t + \nabla \cdot [(h + \zeta)\bar{\mathbf{u}}] = 0 \tag{9}$$

which is exact as no approximation has been introduced in the derivation process. While inaccuracies associated with neglected terms in the momentum equation may be justified by and linked to some frictional effects, higher-order terms, etc. the exactness of mass conservation is essential as there can be no justification of losing or gaining mass in a system. Therefore, the mean velocity, which produces an exact continuity equation in the form of Equation (9), is preferred here.

2.2. Momentum equation

Beji (1998) derived an alternative form of momentum equation for irrotational nonlinear free surface flows, which is exact:

$$\mathbf{u}_t + \nabla\left[g\zeta + \int_z^{\zeta} w_t dz + \frac{1}{2}(\mathbf{u}_\zeta\cdot\mathbf{u}_\zeta + w_\zeta^2)\right] = 0 \qquad (10)$$

where $\mathbf{u}_t$ and w_t are respectively the time derivatives of the horizontal velocity vector and vertical velocity component at an arbitrary depth z while $\mathbf{u}_\zeta$ and w_ζ denote the respective variables evaluated at the free surface ζ. Starting from Equation (10) any kind of depth-integrated wave model may be easily derived once the vertical dependency or the $z-$ profile of the velocity field is specified. Derivations of classical and highly nonlinear Boussinesq models by the use of Equation (10) were demonstrated in Beji (1998).

Equation (10) is first integrated throughout the entire water column from $z=-h$ to $z=\zeta$:

$$\begin{aligned}&\int_{-h}^{\zeta}\mathbf{u}_t dz + g\int_{-h}^{\zeta}\nabla\zeta dz + \int_{-h}^{\zeta}\nabla\left(\int_z^{\zeta} w_t dz\right)dz\\&+\frac{1}{2}\int_{-h}^{\zeta}\nabla(\mathbf{u}_\zeta\cdot\mathbf{u}_\zeta + w_\zeta^2)dz\\&=0\end{aligned} \qquad (11)$$

Considering again Leibnitz's rule for the first term it is possible to write

$$\frac{\partial}{\partial t}\left(\int_{-h}^{\zeta}\mathbf{u}\,dz\right) = \int_{-h}^{\zeta}\mathbf{u}_t dz + \mathbf{u}_\zeta\zeta_t + \mathbf{u}_{-h}h_t \qquad (12)$$

From the definition in Equation (8) the integral in parentheses is $(h+\zeta)\bar{\mathbf{u}}$. Making use of this definition and then employing Equation (12) in Equation (11) gives

$$\begin{aligned}&\tfrac{\partial}{\partial t}[(h+\zeta)\mathbf{u}] - \mathbf{u}_\zeta\zeta_t - \mathbf{u}_{-h}h_t + g(h+\zeta)\nabla\zeta\\&+\int_{-h}^{\zeta}\nabla\left(\int_z^{\zeta} w_t dz\right)dz + \tfrac{1}{2}(h+\zeta)\nabla(\mathbf{u}_\zeta\cdot\mathbf{u}_\zeta + w_\zeta^2) = 0\end{aligned} \qquad (13)$$

Performing the time differentiation of the first term and dividing the entire equation by $(h+\zeta)$ results in

$$\begin{aligned}&\bar{\mathbf{u}}_t + g\nabla\zeta + \frac{1}{(h+\zeta)}\int_{-h}^{\zeta}\nabla\left(\int_z^{\zeta} w_t dz\right)dz\\&+\frac{1}{2}\nabla(\mathbf{u}_\zeta\cdot\mathbf{u}_\zeta + w_\zeta^2)\\&=0\end{aligned} \qquad (14)$$

where the terms $(\bar{\mathbf{u}}-\mathbf{u}_\zeta)\zeta_t$ and $(\bar{\mathbf{u}}-\mathbf{u}_{-h})h_t$, being multiplications of derivatives, have been neglected according to the usual Boussinesq approximations (see Abbott, 1979, p.53). Note that both $(\bar{\mathbf{u}}-\mathbf{u}_\zeta)$ and $(\bar{\mathbf{u}}-\mathbf{u}_{-h})$ are small second-order quantities since they represent the differences between the mean velocity and the surface velocity, and the mean velocity and the bottom velocity, respectively. The relative smallness of these differences is obvious when it is recalled that the higher-order terms; namely, dispersive and nonlinear terms may be manipulated by using the mean, the surface or any other velocity variable interchangeably.

At present, Equation (14) cannot be pursued further unless the vertical dependency of the velocity field is specified so that the depth integration of the third term can be accomplished. In line with the Boussinesq theory, the velocity variables are expanded in power series in z:

$$\begin{aligned}\mathbf{u}(x,y,z,t) &= \sum_{n=0}^{\infty} z^n\mathbf{u}_n(x,y,t),\\ w(x,y,z,t) &= \sum_{n=0}^{\infty} z^n w_n(x,y,t)\end{aligned} \qquad (15)$$

where the terms $\mathbf{u}_0$ and w_0 for $n=0$ represent the horizontal velocity vector and the vertical velocity component at the still water level $z=0$. Expressions given in Equation (15) must satisfy the kinematic conditions; namely, the continuity equation and the irrotationality condition. Substituting the series expansions of Equation (15) into the continuity equation, Equation (1), and arranging results in

$$\begin{aligned}&(\nabla\cdot\mathbf{u}_0 + w_1) + (\nabla\cdot\mathbf{u}_1 + 2w_2)z\\&+(\nabla\cdot\mathbf{u}_2 + 3w_3)z^2 + \cdots\\&=0\end{aligned} \qquad (16)$$

To satisfy Equation (16) the terms inside the parentheses must vanish separately,

$$\begin{aligned}&w_1 = -\nabla\cdot\mathbf{u}_0, \qquad w_2 = -\frac{1}{2}\nabla\cdot\mathbf{u}_1,\\ &w_3 = -\frac{1}{3}\nabla\cdot\mathbf{u}_2, \qquad \cdots\end{aligned} \qquad (17)$$

Expressions in Equation (15) are now used in the irrotationality condition $\partial u/\partial z = \nabla w$ and the relations obtained in Equation (17) are employed so that

$$\begin{aligned}&(\mathbf{u}_1 - \nabla w_0) + [2\mathbf{u}_2 + \nabla(\nabla\cdot\mathbf{u}_0)]z\\&+[3\mathbf{u}_3 + \frac{1}{2}\nabla(\nabla\cdot\mathbf{u}_1)]z^2 + \cdots\\&=0\end{aligned} \qquad (18)$$

Equation (18) in turn implies the following equalities

$$\begin{aligned}&\mathbf{u}_1 = \nabla w_0, \qquad \mathbf{u}_2 = -\frac{1}{2}\nabla(\nabla\cdot\mathbf{u}_0),\\ &\mathbf{u}_3 = -\frac{1}{6}\nabla(\nabla\cdot\mathbf{u}_1) = -\frac{1}{6}\nabla(\nabla^2 w_0), \qquad \cdots\end{aligned} \qquad (19)$$

Thus, the series expansions that satisfy both the continuity equation and the irrotationality condition can be written as

$$\mathbf{u} = \mathbf{u}_0 + z\nabla w_0 - \frac{1}{2}z^2\nabla(\nabla\cdot\mathbf{u}_0) - \frac{1}{6}z^3\nabla(\nabla^2 w_0) - \cdots \qquad (20)$$

$$w = w_0 - z\nabla\cdot\mathbf{u}_0 - \frac{1}{2}z^2\nabla^2 w_0 + \frac{1}{6}z^3\nabla^2(\nabla\cdot\mathbf{u}_0) - \cdots \qquad (21)$$

The bottom condition as given by Equation (3) must now be incorporated into Equation (20) and

Equation (21). Setting $z = -h$ in both equations gives u_{-h} and w_{-h} respectively. Then, these expressions are used in Equation (3) to obtain

$$w_0 = -h_t - \nabla\cdot(h\mathbf{u}_0) + h\nabla h\cdot(\nabla w_0) + \frac{1}{2}h^2\nabla h \cdot[\nabla(\nabla\cdot\mathbf{u}_0)] + \frac{1}{2}h^2\nabla^2 w_0 + \cdots \quad (22)$$

The above expression for w_0 is used on the right successively so that Equation (22) becomes

$$w_0 = -h_t - \nabla\cdot(h\mathbf{u}_0) - h\nabla h \cdot\{\nabla h_t + \nabla[\nabla(h\mathbf{u}_0)]\} + \frac{1}{2}h^2\nabla h \cdot[\nabla(\nabla\cdot\mathbf{u}_0)] - \frac{1}{2}h^2\nabla^2 h_t + \cdots \quad (23)$$

According to the Boussinesq approximations the terms with derivatives higher than the first in the vertical velocity w are all neglected; therefore, only the first two terms of Equation (23) are kept. In the same vein, the terms containing the second and higher spatial derivatives of the depth are neglected. Discharge of higher depth gradients implies the *mild-slope* approximation, which is maintained throughout the work wherever necessary.

Thus, the horizontal velocity vector from Equation (20) and the vertical velocity from Equation (21) with the aid of the truncated form of Equation (23) are now expressed as follows:

$$\mathbf{u} = \mathbf{u}_0 - z\{\nabla h_t + \nabla[\nabla\cdot(h\mathbf{u}_0)]\} - \frac{1}{2}z^2\nabla(\nabla\cdot\mathbf{u}_0) \quad (24)$$

$$w = -h_t - \nabla\cdot(h\mathbf{u}_0) - z(\nabla\cdot\mathbf{u}_0) \quad (25)$$

Note that the velocity of the bottom movement h_t is directly transmitted to w. Equations (24,25) may be used for constructing a Boussinesq model in terms of the still water level velocity; however, in this work the mean velocity is selected as the velocity variable. It is necessary to express $\mathbf{u}$ and w as functions of $\bar{\mathbf{u}}$ instead of u_0. The procedure is straightforward and can be found in Mei (1989, p. 508). Briefly, Equation (24) is integrated vertically for the entire depth so that $\mathbf{u}$ is expressed as a function of $\mathbf{u}_0$. Then, by successive approximations the equation is inverted to express $\mathbf{u}_0$ as a function of $\mathbf{u}$. Finally, this expression is used in both Equations (24,25) so that u and w are now expressed in terms of $\bar{\mathbf{u}}$:

$$\mathbf{u} = \bar{\mathbf{u}} - \frac{1}{2}(h+2z)\{\nabla h_t + \nabla[\nabla\cdot(h\bar{\mathbf{u}})]\} - \frac{1}{6}(h^2 - 3z^2)\nabla(\nabla\cdot\bar{\mathbf{u}}) \quad (26)$$

$$w = -h_t - \nabla\cdot(h\bar{\mathbf{u}}) - z(\nabla\cdot\bar{\mathbf{u}}) \quad (27)$$

The vertical velocity w as expressed in terms of u in Equation (27) may now be used in Equation (14) to obtain a momentum equation that incorporates the vertical motion of seabed.

$$\bar{\mathbf{u}}_t + g\nabla\zeta + \frac{1}{2}\nabla(\bar{\mathbf{u}}\cdot\bar{\mathbf{u}} + h_t^2) + \frac{1}{6}h^2\nabla(\nabla\cdot\bar{\mathbf{u}}_t) = \frac{1}{2}h\nabla[\nabla\cdot(h\bar{\mathbf{u}})_t] + \frac{1}{2}h\nabla h_{tt} \quad (28)$$

in which $\mathbf{u}_\zeta\cdot\mathbf{u}_\zeta$ has been replaced by $\bar{\mathbf{u}}\cdot\bar{\mathbf{u}}$ in accord with usual Boussinesq approximations. Likewise, w_ζ^2 which is made up of multiplications of derivatives of variables, is neglected in Boussinesq-type equations; here h_t^2, the new part of w_ζ^2 is kept temporarily just to show all the new contributions due to bottom movement. Actually, both $\frac{1}{2}\nabla(h_t^2)$ from the left and $\frac{1}{2}h\nabla[\nabla\cdot(h_t\bar{\mathbf{u}})]$ from the right produce terms containing multiplications of derivatives hence are negligible. The only linear term associated with bottom movement is $\frac{1}{2}h\nabla h_{tt}$ and it is this term alone that makes an appreciable difference as demonstrated later for a hypothetical case. Normally, the effect of this term should be tested against experimental data to confirm its corrective aspects. However, relatively long time records of waves generated by relatively slow bottom motions are scarcely available. Therefore, devising a hypothetical numerical experiment appropriate for the purpose seems presently the only way to examine the effect of this term. Moreover, since the earlier work of Wu (1979) confirms the theoretical correctness of $\frac{1}{2}h\nabla h_{tt}$ it would be fair to expect that the inclusion of this term would indeed result in more accurate modeling of waves.

Equations (9,28) in the absence of $\frac{1}{2}\nabla(h_t^2)$ term are in complete agreement with the so-called "generalized Boussinesq" or gB model recapitulated in Wu (2001). The procedure introduced in the present work is relatively short due to use of Equation (10) as the starting point, and it has the advantage of offering the possibility of developing a highly nonlinear[1] Boussinesq model with considerable economy in the terms involved. Specifically, as a part of an iterative numerical scheme, the terms $\mathbf{u}_\zeta$, $\mathbf{u}_{-h}$ and w_ζ may be separately computed from Equations (26,27), and then used in Equation (13). This way all the omitted nonlinear terms can be kept. On the other hand, it must be pointed out that weakly nonlinear theories are satisfactory enough to model nonlinearities in practical applications as indicated by Stiassnie (2017) based on the work of Bonnefoy et al. (2016). Therefore, the lowest order nonlinearity as retained here according to the classical approach is deemed quite appropriate for all practical purposes.

3. Improved Boussinesq model

The Boussinesq-type momentum equation derived for spatially and temporally varying bottom is now

[1]Some Boussinesq models are incorrectly termed as "fully" nonlinear while in essence no wave model based on truncated series expansions can be fully nonlinear.

manipulated to produce a wave model with better dispersion characteristics. The technique, which is called *partial replacement*, is simple and straightforward: a zero addition to dispersion terms and then replacement of parts of the terms by using a zeroth-order relationship (Beji and Nadaoka, 1996). After discharging the negligible contributions $\frac{1}{2}\nabla(h_t^2)$ and $\frac{1}{2}h\nabla[\nabla\cdot(h_t\bar{\mathbf{u}})]$ of bottom movement, by a simple addition and substraction process Equation (28) can be rewritten as

$$\bar{\mathbf{u}}_t+g\nabla\zeta+\tfrac{1}{2}\nabla(\bar{\mathbf{u}}\cdot\bar{\mathbf{u}})+\tfrac{1}{6}(1+\beta)h^2\nabla(\nabla\cdot\bar{\mathbf{u}}_t)-\tfrac{1}{6}\beta h^2\nabla(\nabla\cdot\bar{\mathbf{u}}_t)$$
$$=\tfrac{1}{2}(1+\beta)h\nabla[\nabla\cdot(hu_t)]-\tfrac{1}{2}\beta h\nabla[\nabla\cdot(hu_t)]+\tfrac{1}{2}h\nabla h_{tt} \tag{29}$$

where β is a non-dimensional parameter which is determined in relation to the dispersion relationship of the wave model. As it is permissible to modify the nonlinear and dispersion terms by using the zeroth-order relations the dispersion terms proportional to β are now replaced by their zeroth-order equivalent using $\bar{\mathbf{u}}_t=-g\nabla\zeta$ so that Equation (29) becomes

$$\bar{\mathbf{u}}_t+g\nabla\zeta+\tfrac{1}{2}\nabla(\bar{\mathbf{u}}\cdot\bar{\mathbf{u}})+\tfrac{1}{6}(1+\beta)h^2\nabla(\nabla\cdot\bar{\mathbf{u}}_t)+\tfrac{1}{6}\beta gh^2\nabla(\nabla^2\zeta)$$
$$=\tfrac{1}{2}(1+\beta)h\nabla[\nabla\cdot(h\bar{\mathbf{u}}_t)]+\tfrac{1}{2}\beta gh\nabla[\nabla\cdot(h\nabla\zeta)]+\tfrac{1}{2}h\nabla h_{tt} \tag{30}$$

which is a momentum equation with *mixed* dispersion terms for spatially and temporally varying bathymetry. If the last term is removed, Equation (30) becomes identical with the momentum equation of Beji and Nadaoka (1996). The last term, originating from spatial variations of bed accelerations, acts similar to a dispersion term and smooths out surface fluctuations induced by bottom movement.

For only spatially varying depth $\beta=0$ recovers Peregrine (1967) equations while for constant depth $\beta=-1$ implies original Boussinesq (1872) derivation. For $\beta=1/5$ the linear dispersion relation of the complete set of equations, Equation (9,30), corresponds to the fourth-order Padé approximation of linear theory dispersion relation. The extended applicable range of relative depths for the improved set of equations was explored in detail in Beji and Nadaoka (1996). An in-depth analysis of linear shoaling characteristics of various Boussinesq models, including the present one, can be found in Simarro, Orfila, and Galan (2013).

4. Numerical simulations

Hammack (1973) investigated the transitional bed motions in relation to the surface wave signature and observed that especially for creeping or relatively slow bed motions the time-displacement history of the bed movement influences the surface wave forms appreciably. For determining the relative rapidity of ground motions Hammack (1973) suggested a time-size ratio $t_c\sqrt{gh}/b$, which was later named as the Hammack number (Watts, 2000), where t_c is the characteristic time indicating the duration of bed motion, h is the water depth, b is the width of the uplift or downthrow region, and g is the gravitational acceleration. Impulsive bed motions are categorized as motions with $Ha=t_c\sqrt{gh}/b\ll 1$, transitional bed motions with $Ha=t_c\sqrt{gh}/b\approx 1$, and creeping bed motions with $Ha=t_c\sqrt{gh}/b\gg 1$. The Hammack number may be adapted to underwater landslides by setting t_c to the total duration of landslide as is done in §4.2.

Todorovska and Trifunac (2001) drew attention to a different bed movement duration: the relatively longer duration of long source times resulting from multiplicity of the earthquake source. In such cases faulting does not happen as a single event but in sections: ruptures occur as successive events with delays in between thus producing slow earthquakes or landslides. As the source moves progressively it causes piling up of the surface deformation thus amplifies the waves generated. Considering the study by Abe (1979) of 65 large tsunamigenic seaquakes which occurred between 1837 and 1974, Todorovska and Trifunac (2001) examined the reasons for abnormally large tsunami run-up values; namely, one to two orders of magnitude larger than the average trend values. Among some other factors it has been suggested that such extreme occurrences are caused by a long faulting process or a slow seaquake. This particular point is quite important in the sense that similar to underwater landslides or slumps slow seaquakes may generate larger than expected waves and runup values due to relatively slow bed motions. Then, modeling the surface displacements in accord with the time evolution of the seaquake or landslide becomes crucial for reliable predictions (Hammack, 1973; Løvholt et al., 2015).

4.1. Impulsive upthrust of a bed

Hammack (1973) conducted a series of experiments in a wave tank with a bottom wave generator (bed unit) located at the upstream end of the tank. Among other measurements the downstream wave forms were recorded for an exponential rise of the bed unit. For this particular experiment the relevant parameters were given as $\zeta_0/h=0.1$, $b/h=12.2$, and $t_c\sqrt{gh}/b=0.148$ with ζ_0 denoting the maximum vertical rise of the unit. Rest of the variables have already been defined. The time-size ratio $Ha=0.148$, being considerably less than unity, indicates an impulsive bed motion.

The numerical solution of the new Boussinesq model, Equations (9,30) for $\beta=1/5$, was carried out by the scheme described in detail in Bayraktar and Beji (2013) with the inclusion of newly introduced terms: h_t in the continuity equation and $\frac{1}{2}h\nabla h_{tt}$ in the momentum equation. While the contribution of improved dispersion could be observed quite clearly when simulation was repeated for $\beta = 0$, the contribution of $\frac{1}{2}h\nabla h_{tt}$ is negligible for impulsive bed motions. Its effect is appreciable only for slow or creeping-type bed motions and for these cases measurements are very scarce. Therefore, to reveal the contribution of $\frac{1}{2}h\nabla h_{tt}$ a hypothetical case of relatively slow bed motion is considered in § 4.2.

The simulation exactly imitated the actual physical experiment and a bed unit of total width $b = 0.61$ m (the larger bed unit of the experiments) was placed at the upstream end of the domain with no reflection (solid wall) condition at $x = 0$. The portion of computational domain bed corresponding to the physical bed unit was moved up in exponentially varying fashion, mathematically described in line with Hammack (1973) as

$$h(x,t) = \zeta_0[1 - \exp(-\alpha t)]H(x - b) \qquad (t \geq 0) \quad (31)$$

where $H(x)$ is the Heaviside step function and $\alpha = 1.11/t_c$ so that the bed elevation rises to $2\zeta_0/3$ in t_c second. $h(x,t)$ continues to rise at the same rate in time till it exponentially approaches the maximum elevation ζ_0.

The spatial resolution in the $x-$direction was set to $\Delta x = 0.007$ m and the temporal resolution was $\Delta t = 0.01$ s hence the Courant number $Cr = C(\Delta t/\Delta x)$ was unity for $C = \sqrt{gh}$ with $h = 0.05$ m. From the numerical stability point of view there was no requisite for $Cr = 1$ but was preferred for minimizing phase errors. Since the experiment was physically two dimensional (numerically one dimensional) Δy was arbitrarily selected as 1 m.

Figure 1 compares time histories of measured and computed surface displacement for two different locations: *(a)* at the edge of the bed unit $x = b$, and *(b)* at 20 water depths downstream of the unit $x = b + 20h$. Simulation agrees with measurements quite well, establishing confidence for the model equations and numerical scheme for impulsive bed motions.

4.2. Underwater slump sliding down over a slope

Time domain measurements of waves generated by underwater movements are scarce, measurements with slow bed motions are even scarcer. Since relatively slow bed motions are more influential in subsequent development of surface deformations a hypothetical case is created so that the dispersive effect of bottom acceleration could be observed. Thus, an ellipsoidal underwater slump moving down on an inclined plane is considered for a sample simulation.

The length and width of the simulation domain are 1200 m and 600 m, respectively. The water depth at the beginning of the domain is 2 m and increases to 10 m on a 1 : 75 downslope in the first 600 m distance, while it remains constant at 10 m in the second half of the domain. The slump is in the shape of a half ellipsoid with $z-$axis pointing normal to the inclined plane bed. The length of the primary $x-$axis of the ellipsoid is 120 m and of the primary $y-$axis is 150 m. The maximum height of the slump, or the $z-$axis height of the ellipsoid is 0.5 m. The slump enters the domain at the initial velocity $V_0 = 5\,m/s$ and then keeps speeding under reduced gravitational acceleration $g' = g(\rho_c - \rho_w)/\rho_c \simeq 0.44g$ where $\rho_w = 1025\,kg/m^3$ is the seawater density and $\rho_c = 1826\,kg/m^3$ is the density of wet excavated clay. Theoretical velocity of a material sliding down over an inclined plane of slope angle θ under the action of reduced gravity without friction may be taken as $V(t) = V_0 + (g' \sin\theta)t$. Here, V_0 is the initial velocity of the landslide, $g' \sin\theta$ is the reduced gravitational acceleration acting parallel to the inclined plane, and t is the time. Once the slump reaches the bottom it continues moving at the speed it has attained at the

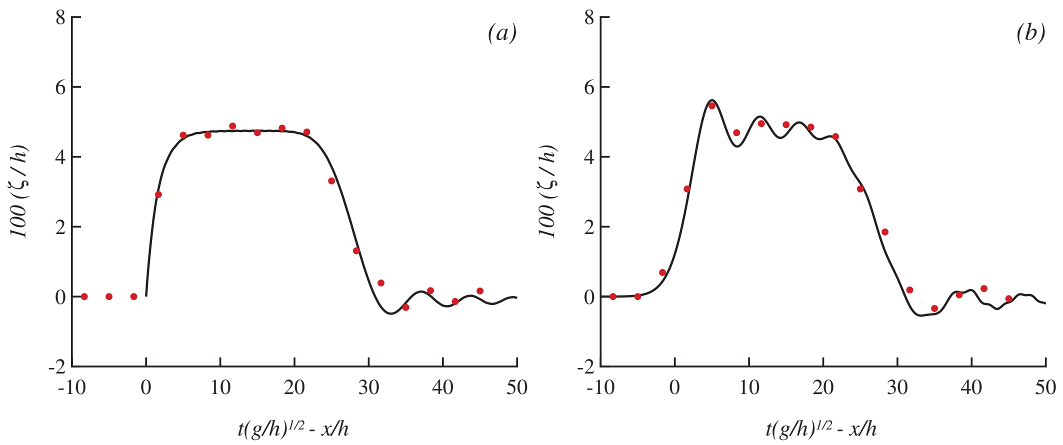

Figure 1. Time history comparisons of Hammack's measurements (red circles) with numerical simulation (solid line) for an impulsive bed upthrust. (a): At the edge of the bed unit $(x - b)/h = 0$, (b): at 20 water depths downstream of the unit $(x - b)/h = 20$.

end of the downslope, which in the present case is nearly 9.7 m/s. This velocity is intentionally arranged to be quite close to the non-dispersive wave celerity at 10 m water depth, $C = \sqrt{gh} = 9.9\,\mathrm{m}/s$ so that the simulation would nearly be for the critical Froude number $Fr = V/C = 1$. An estimate for the relative rapidity of motion can be made by adapting the Hammack number to the present case. Considering the present simulation, the total travel duration of the slump is taken approximately as $t_c = 100\,\mathrm{s}$ while the average shallow water wave velocity is computed by using the mean water depth $h_m = (2 + 10)/2 = 6\,\mathrm{m}$ so that $\sqrt{gh_m} = \sqrt{9.81 \cdot 6} = 7.7\,\mathrm{m}/s$ and the width of the slump $b = 150$ m gives for the time-size ratio or the Hammack number $Ha = 100 \cdot 7.7/150 \approx 5$, which is considerably greater than unity, hence indicating a creeping-type motion.

In the numerical solution the spatial resolutions were taken as $\Delta x = \Delta y = 2\,\mathrm{m}$ while temporal resolution was $\Delta t = 0.2\,\mathrm{s}$. With these resolutions, using the non-dispersive wave celerity at 10 m water depth as representing the wave propagation velocity, the Courant number in both directions $Cr = C(\Delta t/\Delta x) = C(\Delta t/\Delta y)$ was nearly unity. As for the impulsive bed motion simulation it was not necessary to have $Cr = 1$ but was preferred for minimizing phase errors.

Although simplified, the approach used here is sufficiently realistic to produce a hypothetical underwater landslide. Similar approximations are introduced for such hypothetical simulations (Wu, 1987; Dutykh et al., 2013; Dutykh and Kalisch, 2013) and even for actual case scenarios (Løvholt, Pedersen, and Gisler, 2008). The approximations are acceptable in the sense that all these simulations are mere scenarios and actual occurrences cannot be conceived precisely.

Figure 2 shows four different instances; $t = 35\,\mathrm{s}$, $t = 60\,\mathrm{s}$, $t = 85\,\mathrm{s}$, and $t = 110\,\mathrm{s}$, respectively from upper left to lower right, of the location of the hypothetical underwater landslide and corresponding surface deformation. As the slump on the bottom moves, a rise resembling the rooster tail behind a fast-moving vessel develops on the surface and grows. At $t = 110\,\mathrm{s}$ the rooster tail is seen to gain considerable height. Depending on the ratio of the hump speed to the surface wave speed or the Froude number $Fr = V/C = V/\sqrt{gh}$ the overall shape of the surface deformation, wave height, and location of the tail show considerable variations. More specifically, the wave pattern is characterized by the Froude number being equal to unity $Fr = 1$ (critical), greater than unity $Fr > 1$ (supercritical) or less than unity $Fr < 1$ (subcritical). In this example, as indicated before, the Froude number is approximately unity $Fr = 9.7/9.9 = 0.98$ in the constant depth region since the hump speed is nearly the same as the non-dispersive wave celerity hence the flow is critical.

Figure 3 gives the wave profiles along the centerline of domain at the indicated four different instances with and without $\frac{1}{2}h\nabla h_{tt}$. The vertical scale is normalized by the maximum hump height, 0.5 m. Note that the total surface displacement between the minimum and maximum (wave height) becomes as much as 6 times the hump height. The effect of $\frac{1}{2}h\nabla h_{tt}$, which is similar to dispersion, is most clearly observed from the comparison at $t = 110\,\mathrm{s}$. The difference in maximum wave height is nearly 20%, which indicates a definitely non-negligible effect of $\frac{1}{2}h\nabla h_{tt}$ in the computations. From the physical point of view the corrective effect of this particular term may be argued as follows. Spatial variations of bottom acceleration necessarily spread the created surface disturbance over a wider region thus smearing or softening the sharper wave forms. The same behavior is observed for dispersion which counterbalances the

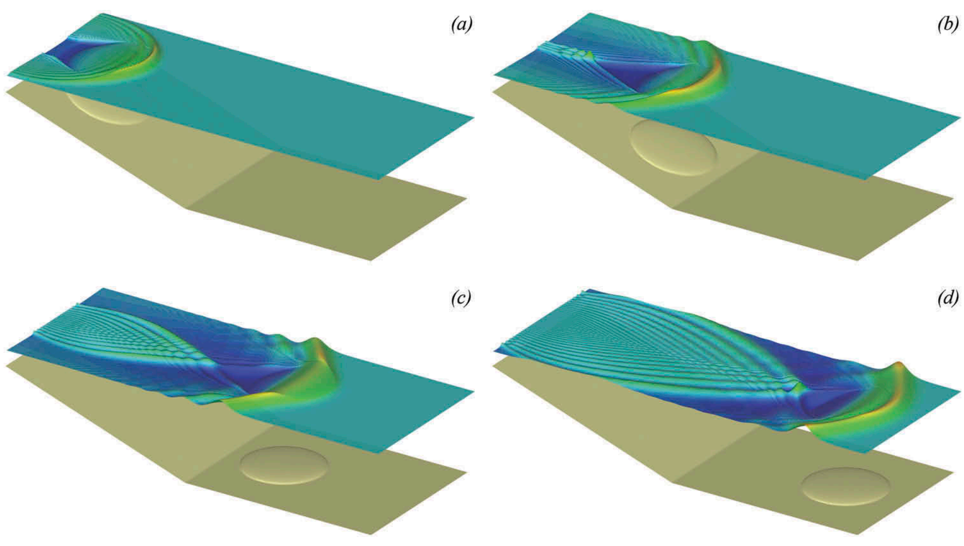

Figure 2. Location of the hypothetical underwater landslide and corresponding surface deformation for four different instances: (a): $t = 35\,\mathrm{s}$, (b): $t = 60\,\mathrm{s}$, (c): $t = 85\,\mathrm{s}$, and (d): $t = 110\,\mathrm{s}$.

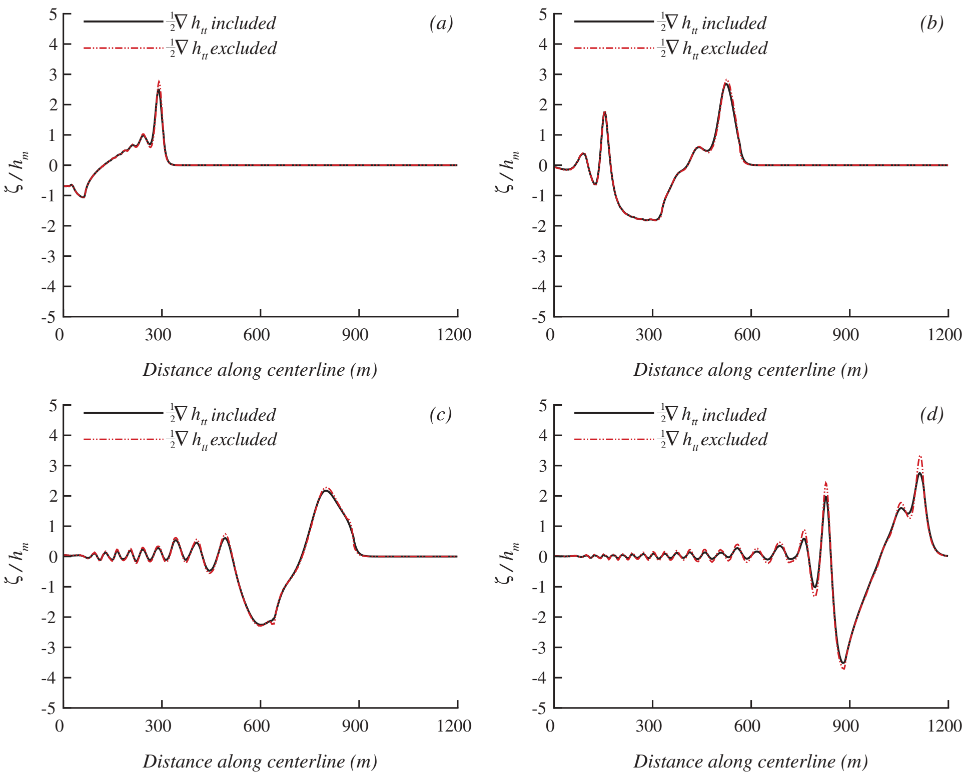

Figure 3. Surface deformations along the centerline at four different instances (a): $t = 35$ s, (b): $t = 60$ s, (c): $t = 85$ s, and (d): $t = 110$ s. Solid line: computation with $\frac{1}{2}h\nabla h_{tt}$, red dash–dash–dot line: computation without $\frac{1}{2}h\nabla h_{tt}$.

steepening of wave forms due to sheer nonlinearity. Then, the presently computed reduction in wave height is actually an anticipated and expected feature caused by spatial variations in accelerative bottom movements.

5. Concluding remarks

A Boussinesq-type wave model comprising time-dependent bottom variations has been derived. The model equations contain not only the usual bottom velocity h_t in the continuity equation but also three new terms with time-dependent depth variations in the momentum equation. These new terms are the nonlinear contribution $\frac{1}{2}\nabla(h_t^2)$, the high-order dispersion term associated with bottom velocity $\frac{1}{2}h\nabla[\nabla \cdot (h_t u)]$, and finally the linear contribution involving bottom acceleration $\frac{1}{2}h\nabla h_{tt}$. Although the first two terms would usually be negligible, the last term $\frac{1}{2}h\nabla h_{tt}$, being linear, makes appreciable corrections to the wave height (around 20% for the sample case) hence must be included for reliable calculations. Still, it should be pointed out h_t in the continuity equation is the main zeroth-order linear contribution, which generates the surface motion.

The new set of equations, being also capable of modeling relatively shorter waves due to improved dispersion capabilities, may be used for convenient and accurate modeling of surface waves generated especially by underwater slides or piecewise faulting slow seaquakes. Convenience is due to the use of the same set of equations instead of combining different models for wave-generation and far-field propagation as for instance in Løvholt, Pedersen, and Gisler (2008). Accuracy is basically achieved by both the improved dispersion characteristics of the model allowing relatively shorter wave propagation and the inclusion of corrective term $\frac{1}{2}h\nabla h_{tt}$ for better wave height estimation.

Disclosure statement

No potential conflict of interest was reported by the author.

ORCID

S. Beji http://orcid.org/0000-0002-1927-9262

References

Abbott, M. B. 1979. *Computational Hydraulics: Elements of the Theory of Free Surface Flows*. London: Pitman.

Abe, K. 1979. “Size of Great Earthquakes of 1837–1974 Inferred from Tsunami Data.” *Journal of Geophysical Research* 84 (B4): 1561–1568. doi:10.1029/JB084iB04p01561.

An, C., I. Sepúlveda, and P. L.-F. Liu. 2014. “Tsunami Source and Its Validation of the 2014 Iquique, Chile Earthquake.” *Geophysical Research Letters* 41: 3988–3994. doi:10.1002/2014GL060567.

Bayraktar, D., and S. Beji. 2013. “Numerical Simulation of Waves Generated by a Moving Pressure Field.” *Ocean Engineering* 59: 231–239. doi:10.1016/j.oceaneng.2012.12.025.

Beji, S. 1998. "Note on Conservation Equations for Nonlinear Surface Waves." *Ocean Engineering* 25 (7): 607–613.

Beji, S., and K. Nadaoka. 1996. "A Formal Derivation and Numerical Modelling of the Improved Boussinesq Equations for Varying Depth." *Ocean Engineering* 23 (8): 691–704. doi:10.1016/0029-8018(96)84408-8.

Bonnefoy, F., F. Haudin, G. Michel, B. Semin, T. Humbert, S. Aumaître, M. Berhanu, and E. Falcon. 2016. "Observation of Resonant Interactions among Surface Gravity Waves." *Journal Fluid Mechanisms* 805 (R3): 1–12. doi:10.1017/jfm.2016.576.

Boussinesq, J. V. 1872. "Théorie des Ondes et des Remous Qui se Propagent le Long d'un Canal Rectangulaire Horizontal, en Communiquant au Liquide Contenu dans ce Canal des Vitesses Sensiblement Pareilles de la Surface au Fond." *Journal Mathematical Pures Applications 2nd Series* 17: 55–108.

Dutykh, D., D. Mitsotakis, S. Beysel, and N. Shokina. 2013. "Dispersive Waves Generated by an Underwater Landslide." In *Numerical Methods for Hyperbolic Equations Theory and Applications*. Santiago de Compostela, Spain: CRC Press (pp. 245–250).

Dutykh, D., and H. Kalisch. 2013. "Boussinesq Modeling of Surface Waves Due to Underwater Landslides." *Nonlinear Processes in Geophysics* 20: 267–285. doi:10.5194/npg-20-267-2013.

Fritz, H. M., W. H. Hager, and H.-E. Minor. 2004. "Near Field Characteristics of Landslide Generated Impulsive Waves." *Journal of Waterway, Port, Coastal, and Ocean Engineering* 130 (6): 287–302. doi:10.1061/(ASCE)0733-950X(2004)130:6(287).

Goto, C., Y. Ogawa, and F. Imamura. 1997. "Numerical Method of Tsunami Simulation with the Leap-Frog Scheme." *IUGG/IOC Time Project, IOC Manuals and Guides* 35. UNESCO.

Hammack, J. L. 1973. "A Note on Tsunamis: Their Generation and Propagation in an Ocean of Uniform Depth." *Journal Fluid Mechanisms* 60: 769–799. doi:10.1017/S0022112073000479.

Horrillo, J., Z. Kowalik, and Y. Shigihara. 2006. "Wave Dispersion Study in the Indian Ocean-Tsunami of December 26, 2004." *Marine Geodesy* 29: 149–166. doi:10.1080/01490410600939140.

Kowalik, Z., and T. Logan. 2005. "Numerical Modeling of the Global Tsunami: Indonesian Tsunami of 26 December 2004." *Science of Tsunami Hazards* 23 (1): 40–56.

Løvholt, F., G. Pedersen, C. B. Harbitz, S. Glimsdal, and J. Kim. 2015. "On the Characteristics of Landslide Tsunamis." *Philosophical Transactions of the Royal Society A* 373 (20140376): 1–18. doi:10.1098/rsta.2014.0376.

Løvholt, F., G. Pedersen, and G. Gisler. 2008. "Oceanic Propagation of a Potential Tsunami from the La Palma Island." *Journal of Geophysical Research* 113 (C09026): 1–21. doi:10.1029/2007JC004603.

Madsen, P. A., and H. A. Schäffer. 1998. "Higher-Order Boussinesq-Type Equations for Surface Gravity Waves: Derivation and Analysis." *Philosophical Transactions of the Royal Society London A* 356: 3123–3184. doi:10.1098/rsta.1998.0309.

Madsen, P. A., and O. R. Sørensen. 1992. "A New Form of the Boussinesq Equations with Improved Linear Dispersion Characteristics: Part 2. A Slowly-Varying Bathymetry." *Coastal Engineering* 8: 183–204. doi:10.1016/0378-3839(92)90019-Q.

Madsen, P. A., R. Murray, and O. R. Sørensen. 1991. "A New Form of the Boussinesq Equations with Improved Linear Dispersion Characteristics." *Coastal Engineering* 15: 371–388. doi:10.1016/0378-3839(91)90017-B.

Mei, C. C. 1989. *The Applied Dynamics of Ocean Surface Waves*. Singapore: World Scientific.

Mei, C. C., and B. Le Méhauté. 1966. "Note on the Equations of Long Waves over an Uneven Bottom." *Journal of Geophysical Research* 71: 393–400. doi:10.1029/JZ071i002p00393.

Nagano, O., F. Imamura, and N. Shuto. 1991. "A Numerical Model for Far-Field Tsunamis and Its Application to Predict Damages Done to Aquaculture." *Natural Hazards* 4: 235–255. doi:10.1007/BF00162790.

Nwogu, O. 1993. "Alternative Form of Boussinesq Equations for Nearshore Propagation." *Journal Waterway, Port, Coastal, and Ocean Engineering* 9 (6): 618–638. doi:10.1061/(ASCE)0733-950X(1993)119:6(618).

Peregrine, D. H. 1967. "Long Waves on a Beach." *Journal Fluid Mechanisms* 27: 815–827. doi:10.1017/S0022112067002605.

Shuto, N. 1991. "Numerical Simulation of Tsunamis – Its Present and near Future." *Natural Hazards* 4: 171–191. doi:10.1007/BF00162786.

Simarro, G., A. Orfila, and A. Galan. 2013. "Linear Shoaling in Boussinesq-Type Wave Propagation Models." *Coastal Engineering* 80: 100–106. doi:10.1016/j.coastaleng.2013.05.009.

Stiassnie, M. 2017. "On the Strength of the Weakly Nonlinear Theory for Surface Gravity Waves." *Journal Fluid Mechanisms* 810: 1–4. doi:10.1017/jfm.2016.632.

Titov, V., U. Kanoglu, and C. Synolakis. 2016. "Development of MOST for Real-Time Tsunami Forecasting." *Journal Waterway, Port, Coastal, and Ocean Engineering* 142 (6): 1–16. 03116004. doi:10.1061/(ASCE)WW.1943-5460.0000357.

Todorovska, M. I., and M. D. Trifunac. 2001. "Generation of Tsunamis by a Slowly Spreading Uplift of the Sea Floor." *Soil Dynamics and Earthquake Engineering* 21: 151–167. doi:10.1016/S0267-7261(00)00096-8.

Watts, P. 2000. "Tsunami Features of Solid Block Underwater Landslides." *Journal of Waterway, Port, Coastal, and Ocean Engineering* 126 (3): 144–152. doi:10.1061/(ASCE)0733-950X(2000)126:3(144).

Witting, J. M. 1984. "A Unified Model for the Evolution of Nonlinear Water Waves." *Journal of Computational Physics* 56: 203–236. doi:10.1016/0021-9991(84)90092-5.

Wu, T. Y. 1979. "On Tsunami Propagation: Evaluation of Existing Models." In *Tsunamis–Proceeding of National Science Foundation Workshop*. Pasadena, CA.

Wu, T. Y. 1981. "Long Waves in Ocean and Coastal Waters." *Journal of Engineering Mechanics Div ASCE* 107: 501–522.

Wu, T. Y. 1987. "Generation of Upstream Advancing Solitons by Moving Disturbances." *Journal Fluid Mechanisms* 184: 75–99. doi:10.1017/S0022112087002817.

Wu, T. Y. 2001. "A Unified Theory for Modeling Water Waves." *Advancement Applications Mechanisms* 37: 1–88.

Yamazaki, Y., K. F. Cheung, and Z. Kowalik. 2010. "Depth-Integrated, Non-Hydrostatic Model with Grid Nesting for Tsunami Generation, Propagation, and Run-Up." *International Journal Numerical Methods Fluids* 67: 2081–2107. doi:10.1002/fld.2485.